Small-signal modelling of AC/MTDC hybrid power systems using Multi-Layer Component Connection Method

Wang, Hao; Hu, Weihao; Zhang, Guozhou; Tang, Yuanhong; Jing, Shi; Chen, Zhe

Published in:
Energy Reports

DOI (link to publication from Publisher):
10.1016/j.egyr.2020.11.080

Publication date:
2020

Document Version
Publisher's PDF, also known as Version of record

Citation for published version (APA):
Wang, H., Hu, W., Zhang, G., Tang, Y., Jing, S., & Chen, Z. (2020). Small-signal modelling of AC/MTDC hybrid power systems using Multi-Layer Component Connection Method. *Energy Reports*, *6*(Suppl. 9), 1033-1040. https://doi.org/10.1016/j.egyr.2020.11.080

Available online at www.sciencedirect.com

ScienceDirect

Energy Reports 6 (2020) 1033–1040

www.elsevier.com/locate/egyr

2020 7th International Conference on Power and Energy Systems Engineering (CPESE 2020), 26–29 September 2020, Fukuoka, Japan

Small-signal modelling of AC/MTDC hybrid power systems using Multi-Layer Component Connection Method

Hao Wang[a,b], Weihao Hu[a,*], Guozhou Zhang[a], Yuanhong Tang[a], Shi Jing[a], Zhe Chen[b]

[a] *School of Mechanical and Electrical Engineering, University of Electronic Science and Technology of China, Chengdu, China*

[b] *Department of Energy Technology, Aalborg University, Aalborg, Denmark*

Received 26 October 2020; accepted 11 November 2020

Abstract

In order to simplify the stability analysis of an AC/MTDC (multi-terminal direct current) power system, this paper presents a Multi-Layer Component Connection Method (MLCCM)-based small signal model for AC/MTDC hybrid power systems. Based on ML-CCM, the system is partitioned as small individual system or components, including generator units, voltage source converter (VSC) units, time delay units, AC network and DC network. The modelling procedure can be 3 steps. First, the individual components are independently modelled. Second, several small individual components are assembled together to build the AC system model based on component interconnection relationship. Third, all AC power systems and DC network model are assembled together to build the whole hybrid power based on the interconnection relationship. There are three features for the MLCCM: (1) these component models can be built individually; (2) their interconnection relationship is a linear algebra matrix; (3) subsystem model can be verified or debugged individually. Due to the three features, the whole hybrid power can be built easily and it is convenient for finding modelling fault and debugging. An AC/DC hybrid system model in MATLAB/Simulink is also built to validate the effectiveness of the MLCCM-based small signal model.

Peer-review under responsibility of the scientific committee of the 7th International Conference on Power and Energy Systems Engineering, CPESE, 2020.

Keywords: MTDC; Component Connection Method; Small signal model; VSC

1. Introduction

Over the last decades, Voltage source converter (VSC) based multi-terminal direct current (MTDC) systems have become a hot topic [1]. It is one of the most promising methods to integrate non-synchronous AC grids into one AC/DC hybrid system. The first commercial operational high voltage direct current (HVDC) system, HVDC Italy-Corsica-Sardinia, was built in 1988 [2]. With the increasing of availability and cost-efficiency of VSCs, VSC-MTDC has become an available solution for renewable energy integration and power transmission [2]. In China,

* Corresponding author.
E-mail address: whu@uestc.edu.cn (W. Hu).

https://doi.org/10.1016/j.egyr.2020.11.080

Peer-review under responsibility of the scientific committee of the 7th International Conference on Power and Energy Systems Engineering, CPESE, 2020.

the operating MTDC projects are built for wind power powering islands and transmission, such as Zhoushan VSC-MTDC project and Nanao VSC-MTDC project, In Europe, for off-shore wind power transmission, a pan-European supergrid project is proposed [2].

With the increasing installations of VSC-HVDC in power grids, the investigation of stability and control method of MTDC systems becomes more and more important for the existing power systems. Therefore, it is necessary to build the mathematical model to evaluate the stability problems. Reasonable selection of control parameters may effectively improve system damping characteristics and reduce the risks of operational failure or oscillation. Time-domain simulation may assist with parameters selection. However, Small signal stability analysis for power system is usually carried out instead of time-domain simulation [3].

The conventional state–space small signal model of VSC-MTDC was used in [4–7]. The conventional state-space approach tends to formulate a very high order state matrix and result in a complicated modelling procedure. The impedance-based method is another effective way to analyse small signal stability. Nevertheless, the impedance-based method is difficult to be extended to multi-inverter DC systems [8].

To overcome the above-mentioned limitations, this paper presents a Multi-Layer Component Connection Method-based (MLCCM) state-space small signal model, which combines the advantages of general state-space-based model and impedance-based method. The CCM is a simplified approach of state space modelling [9,10]. The CCM was ever introduced to investigate the dynamic stability of inverter-fed AC power system [9]. In this work, the idea of Multi-Layer is combined with CCM to build small signal model for AC/MTDC hybrid power system. Compared with the conventional state-space method, the advantages of MLCCM are: (1) the modelling procedure is simple; (2) It is easy for a system to extend subsystems by modular modelling procedure; (3) It is convenient to find modelling fault and debug. This method provides plug-and-play flexibility for state-space small signal model.

The rest of this paper is organized as follows. In Section 2, the principle of MLCCM is described. The detailed MLCCM-based modelling procedure is given in Section 3. The simulation results are presented to validate the modelling method in Section 4. The conclusions are drawn in Section 5.

2. System description and Multi-Layer Component Connection Method

This section describes the structure of an AC/MTDC hybrid power system and the Multi-Layer Component Connection Method (MLCCM).

2.1. System description

With a radial topology, a four-terminal DC system is shown in Fig. 1(a), which will be analysed as an example in this work. In this hybrid system, four nonsynchronous AC grids are connected to the HVDC system by four VSC stations, which is marked as Converter 1, 2, 3 and 4 respectively. In the DC system, the VSC stations are connected to the centre node (Node 5) through four resistances: R_1, R_2, R_3 and R_4. In the AC side, four nonsynchronous AC systems 1, 2, 3, 4 are connected to DC grid via Converter 1, 2, 3, 4 respectively. Fig. 1(b) depicts the simplified AC power system topology.

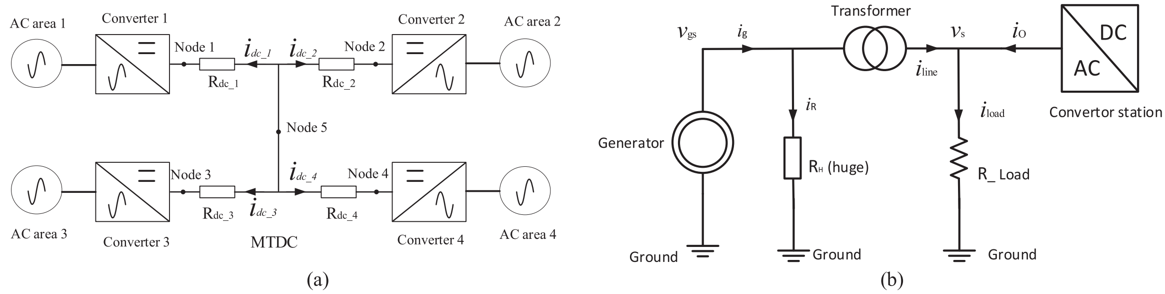

Fig. 1. AC/MTDC hybrid power system. (a) MTDC power system; (b) AC grid.

2.2. Component Connection Method (CCM)

In CCM, each component is modelled independently. Consider the dynamical system of ith component with state model [10].

$$\begin{aligned} \dot{x}_i &= A_i x_i + B_i a_i \\ b_i &= C_i x_i + D_i a_i \end{aligned} \tag{1}$$

Then, all the models are assembled together to form a composite system model as given in (2)

$$\begin{aligned} \dot{x} &= A_T x_T + B_T a_T \\ b_T &= C_T x_T + D_T a_T \end{aligned} \tag{2}$$

where A_T, B_T, C_T, D_T are system matrixes. They are diagonal matrixes.

$A_T = diag(A_1, \ldots, A_i, \ldots, A_n)$, $B_T = diag(B_1, \ldots, B_i, \ldots, B_n)$, $C_T = diag(C_1, \ldots, C_i, \ldots, C_n)$, $D_T = diag(D_1, \ldots, D_i, \ldots, D_n)$.

where $x_T = [x_1, \ldots, x_i, \ldots, x_n]^T$, $a_T = [a_1, \ldots, a_i, \ldots, a_n]^T$, $b_T = [b_1, \ldots, b_i, \ldots, b_n]^T$.

Generally, algebra equations can be used to describe the interconnection relationship of different components.

$$\begin{aligned} a_T &= L_{11} b_T + L_{12} u \\ y &= L_{21} b_T + L_{22} u \end{aligned} \tag{3}$$

where a_T and b_T are component input and output vectors, u and y are inputs and output vectors of composite system.

L_{11}, L_{12}, L_{21}, L_{22}, are the algebra relationship matrixes. The desired state model of composite system can be obtained by combining equation (1)–(3).

$$\begin{aligned} \dot{x}_T &= F x_T + G u \\ y &= H x_T + J u \end{aligned} \tag{4}$$

where $F = A_T + B_T(I - L_{11}D_T)^{-1}L_{11}C_T$, $G = B_T(I - L_{11}D_T)^{-1}L_{12}$, $H = L_{21}(I - D_T L_{11})^{-1}C_T$, $J = L_{21}D_T(I - L_{11}D_T)^{-1}L_{12} + L_{22}$.

Then, the stability of the composite system can be investigated via Eq. (4).

2.3. Multi-Layer Component Connection Method (MLCCM)

Fig. 2 shows the 4 layers of hybrid power system which is corresponding to Fig. 1. The whole system is partitioned into generator, VSC controllers, delay units, AC networks and DC network components. The first layer is the models of each independent components. The second layer is the model of voltage source converter (VSC) which will be built from combining some individual component models. The third layer is the AC grid model and the fourth is the whole hybrid power system model. All the components can be modelled independently. Low layer is subsystem of high layer. Low layer or subsystem model can be verified or debugged individually.

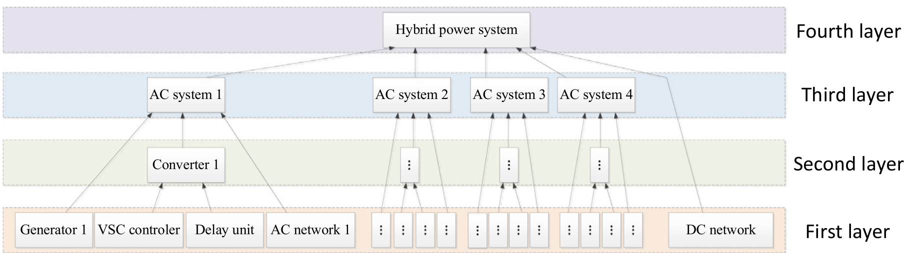

Fig. 2. Diagram of MLCCM-based method.

3. The proposed Multi-Layer Component Connection Method modelling procedure

The proposed MLCCM-based modelling procedure is demonstrated with reference to the exemplified hybrid power system shown in Fig. 1. There are 4 layers for modelling the whole hybrid power system as described in

Fig. 2. The procedure starts from first layer and ends in fourth layer. The models of every layer can be debugged independently. It is convenient for the entire hybrid system to be debugged.

In fact, a 120-order model consisting of 120 state variables will be built for the AC/MTDC power system. There are numerous elements in the state matrix, input matrix, output matrix and feedthrough matrix. However, considering the limit length of this article, these elements will not be demonstrated. The main purpose of this paper is to propose a modelling method. With the description of this paper, the reader can obtain the same state-space model with the model used by this paper.

3.1. First layer: Modelling of each individual component

3.1.1. Component of VSC controller

In order to realize nonsynchronous weak AC power system sharing their frequency assistant function, generally, the AC frequency droop (f-P) control and DC voltage droop (Vdc-P) control will be adopted [11]. This paper adopt the V_{dc}-f droop control as shown in Fig. 3. The reactive power (Q) filter in Fig. 3 is a first order low pass filter with the time constant K_{Qs}.

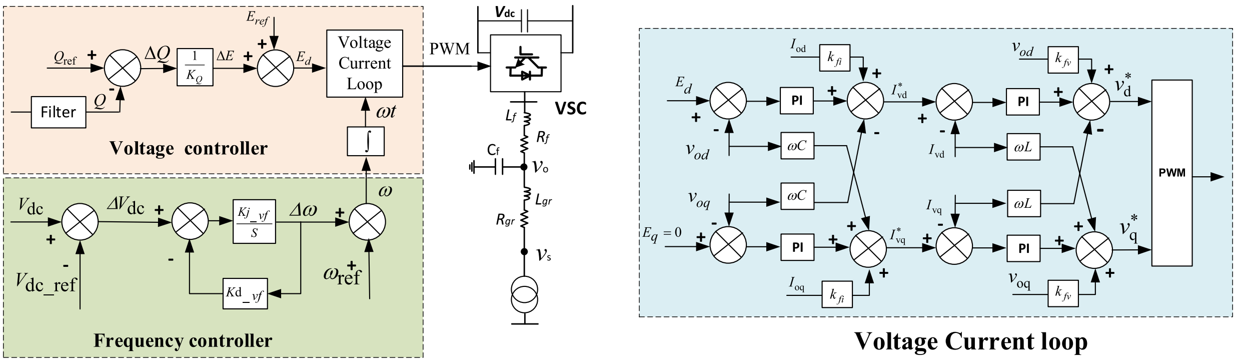

Fig. 3. Diagram of VSC controller.

Based on the control loop and LC filter circuit topology, a twelve-order model consisting of twelve variables can be obtained. The state-space model is built in the dq rotating reference frame.

$$\begin{aligned} \dot{x}_{vsc-c} &= A_{vsc-c}x_{vsc-c} + B_{vsc-c}a_{vsc-c} \\ b_{vsc-c} &= C_{vsc-c}x_{vsc-c} + D_{vsc-c}a_{vsc-c} \end{aligned} \tag{5}$$

where $x_{vsc-c} = \left[\Delta i_{vd}, \Delta i_{vq}, \Delta v_{od}, \Delta v_{oq}, \Delta i_{od}, \Delta i_{oq}, \Delta Q, \Delta\omega, \Delta\gamma_{vd}, \Delta\gamma_{vq}, \Delta\gamma_{cd}, \Delta\gamma_{cq},\right]^T$, $a_{vsc-c} = \left[\Delta v_{vd}, \Delta v_{vq}, \Delta v_{sd}, \Delta v_{sq}, \Delta V_{dc}, \Delta v_{ref}, \Delta Q_{ref}, \Delta v^*_{vd}, \Delta v^*_{vq}\right]^T$ $b_{vsc-c} = \left[\Delta i_{vd}, \Delta i_{vq}, \Delta i_{od}, \Delta i_{oq}, \Delta v^*_{vd}, \Delta v^*_{vq}, \Delta\omega, \Delta v_{vd\_i}, \Delta v_{vq}\right]^T$. $\Delta\gamma_{\mathrm{vd}}$, $\Delta\gamma_{\mathrm{vq}}$, $\Delta\gamma_{\mathrm{cd}}$, $\Delta\gamma_{\mathrm{cd}}$ represent the integral variable in the voltage control loop and current control loop respectively.

3.1.2. Component of generator

In consideration of the tandem-compound reheat turbine and power system stabilizer (PSS) [12], each synchronous generator can be modelled with a nine-order model consisting of nine state variables as follows. The block diagram is shown in Fig. 4.

Then the state–space model of generator can be obtained.

$$\begin{aligned} \dot{x}_g &= A_g x_g + B_g a_g \\ b_g &= C_g x_g + D_g a_g \end{aligned} \tag{6}$$

where $x_g = \left[\triangle\omega_g, \Delta P_m, \Delta P_p, \Delta Y, \Delta\theta_g, \Delta i_{gd}, \Delta i_{gq}, \Delta v_h, \Delta v_g\right]^T$, $a_g = [\Delta\omega_i, \Delta v_{sd}, \Delta v_{sq}, \Delta P_{ref}]^T$, $b_g = [\Delta i_{gd}, \Delta i_{gq}]^T$. In turbine equation, second order derivative of ΔP_{m} exists. In order to solve this problem, ΔP_{p} is introduced as the first derivative of ΔPm. $\Delta\omega$ is the frequency deviation of the VSC, which is in the common AC grid.

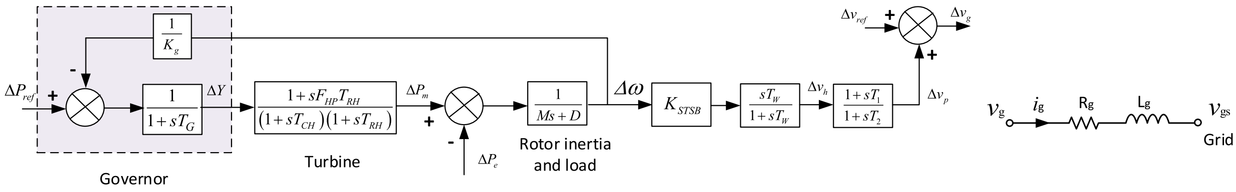

Fig. 4. Diagram of generator model.

3.1.3. Component of time delay unit

According to the third-order Pade approximation, the transfer function of control system delay may be represented by

$$e^{-\tau \cdot s} \approx \frac{1 - 1/2\tau s + 1/10\tau^2 s^2 - 1/120\tau^3 s^3}{1 + 1/2\tau s + 1/10\tau^2 s^2 + 1/120\tau^3 s^3} \tag{7}$$

which can be described as

$$\begin{aligned} \dot{x}_{del} &= A_{\mathrm{del}} x_{del} + B_{del} a_{del} \\ b_{del} &= C_{del} x_{del} + D_{del} a_{del} \end{aligned} \tag{8}$$

where $x_{del} = [\Delta x_{del1d}, \Delta x_{del2d}, \Delta x_{del3d}, \Delta x_{del1q}, \Delta x_{del2q}, \Delta x_{del3q}]^T$, $a_{del} = [v^*_{vd}, v^*_{vq}]^T$, $b_{del} = [v_{vd}, v_{vq}]^T$. (assuming time delay occurs on v^*_{vd} and v^*_{vq} respectively)

3.1.4. Component of AC network

It is assumed that the load is active power load. Base on the ac grid topology shown in Fig. 1(b), a two-order model is built.

$$\begin{aligned} \dot{x}_{AC-net} &= A_{AC-net} x_{AC-net} + B_{AC-net} a_{AC-net} \\ b_{AC-net} &= C_{AC-net} x_{AC-net} + D_{AC-net} a_{AC-net} \end{aligned} \tag{9}$$

where, $x_{AC-net} = [\Delta i_{lined}, \Delta i_{lineq}]^T$, $a_{AC-net} = [\Delta v_{gsd}, \Delta v_{gsq}, \Delta v_{loadd}, \Delta v_{loadq}, \Delta\omega]^T$, $b_{AC-net} = [\Delta i_{lined}, \Delta i_{lineq}]^T$.

3.1.5. Component of DC network

Base on the DC grid topology shown in Fig. 1(a) and Fig. 5, a four-order model is built.

$$\begin{aligned} \dot{x}_{dc} &= A_{dc} x_{dc} + B_{dc} a_{dc} \\ b_{dc} &= C_{dc} x_{dc} + D_{dc} a_{dc} \end{aligned} \tag{10}$$

Where $x_{dc} = [\Delta V_{dc\_1}, \Delta V_{dc\_2}, \Delta V_{dc\_3}, \Delta V_{dc\_4}]^T$, $a_{dc} = [i_1, i_2, i_3, i_4,]^T$, $x_{dc} = [\Delta V_{dc\_1}, \Delta V_{dc\_2}, \Delta V_{dc\_3}, \Delta V_{dc\_4}]^T$.

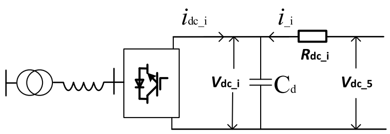

Fig. 5. Diagram of DC circuit.

3.2. Second layer: modelling of VSC

VSC controller models and delay unit models are written together as follow

$$\begin{aligned} \dot{x}_{vsc} &= A_{T-vsc} x_{vsc} + B_{\mathrm{T}-vsc} a_{vsc} \\ b_{vsc} &= D_{T-vsc} x_{vsc} + D_{\mathrm{T}-vsc} a_{vsc} \end{aligned} \tag{11}$$

where $A_{T-vsc} = diag(A_{vsc-c}, A_{del})$, $B_{T-vsc} = diag(B_{vsc-c}, B_{del})$, $C_{T-vsc} = diag(C_{vsc-c}, C_{del})$, $D_{T-vsc} = diag(D_{vsc-c}, D_{del})$, $x_{vsc} = [x_{vsc\_c}, x_{del}]^T$, $a_{vsc} = [a_{vsc\_c}, a_{del}]^T$, $b_{vsc} = [b_{vsc\_c}, b_{del}]^T$. Though the equations of two individual components are written together, there is lack a connection between the two model variables.

Considering, $u_{vsc} = \left[\Delta v_{sd}, \Delta v_{sq}, \Delta V_{dc\_i}, \Delta v_{ref}, \Delta Q_{ref}\right]^T$, $y_{vsc} = \left[\Delta i_{od}, \Delta i_{oq}, \Delta\omega, \Delta i_{vd}, \Delta i_{vq}, \Delta v_{vd}, \Delta v_{vq}\right]^T$ based on the algebra relationship of variables in the a_{vsc}, b_{vsc}, y_{vsc}, it is easy to obtain

$$\begin{aligned} a_{vsc} &= L_{11-vsc}b_{vsc} + L_{12-vsc}u_{vsc} \\ y_{vsc} &= L_{21-vsc}b_{vsc} + L_{22-vsc}u_{vsc} \end{aligned} \tag{12}$$

Eq. (12) is algebra equation.

Based on CCM, the VSC model can be obtained as

$$\begin{aligned} \dot{x}_{vsc} &= F_{vsc}x_{vsc} + G_{vsc}u_{vsc} \\ y_{vsc} &= H_{vsc}x_{vsc} + J_{vsc}u_{vsc} \end{aligned} \tag{13}$$

where $F_{vsc} = A_{T-vsc} + B_{T-vsc}(I - L_{11-vsc}D_{T-vsc})^{-1}L_{11-vsc}C_{T-vsc}$, $G_{vsc} = B_{T-vsc}(I - L_{11-vsc}D_{T-vsc})^{-1}L_{12-vsc}$, $H_{vsc} = L_{21-vsc}(I - D_{T-vsc}L_{11-vsc})^{-1}C_{T-vsc}$, $J_{vsc} = L_{21-vsc}D_{T-vsc}(I - L_{11-vsc}D_{T-vsc})^{-1}L_{12-vsc} + L_{22-vsc}$.

3.3. Third layer: modelling of AC grid

As shown in Fig. 1(b), AC grid model is constituted by generator model, AC network model and VSC model. Based on the same idea and method in part 3.2, the new model can be obtained.

$$\begin{aligned} \dot{x}_{ac} &= F_{ac}x_{ac} + G_{ac}u_{ac} \\ y_{ac} &= H_{ac}x_{ac} + J_{ac}u_{ac} \end{aligned} \tag{14}$$

where, $x_{ac} = [x_g, x_{vsc}, x_{AC-net}]^T$, $u_{ac} = \left[\Delta P_{ref}, \Delta V_{dc}, \Delta v_{ref}, \Delta Q_{ref}\right]^T$, $y_{ac} = \left[\Delta i_{vd}, \Delta i_{vq\_i}, \Delta v_{vd}, \Delta v_{vq}, \Delta\omega\right]^T$.

3.4. Fourth layer: modelling of AC/MTDC hybrid power system

From Fig. 1(a), the entire hybrid power system model is made up of four AC grid models and DC network model. With the same idea and method in part 3.2, the new model can be built. However, the power balance equation (15) must be used to form the algebraic relationship matrix.

$$V_{dc0\_i}\Delta I_{dc\_i} + I_{dc0\_i}\Delta V_{dc\_i} + i_{vd0\_i}\Delta v_{d\_i} + v_{d0\_i}\Delta i_{vd\_i} + i_{vq0\_i}\Delta v_{q\_i} + v_{q0\_i}\Delta i_{vq\_i} = 0 \tag{15}$$

where subscript i denotes variable in ith AC grid or variable connected with ith AC grid. The subscript 0 denotes the initial value of variable.

The state-space model of the entire hybrid power system is shown as follow

$$\begin{aligned} \dot{x}_{entire} &= F_{entire}x_{entire} + G_{entire}u_{entire} \\ y_{entire} &= H_{entire}x_{entire} + J_{entire}u_{entire} \end{aligned} \tag{16}$$

where $x_{entire} = [x_{ac\_1}, x_{ac\_2}, x_{ac\_3}, x_{ac\_4}]^T$, $u_{entire} = \left[\Delta P_{ref\_1}, \Delta v_{ref\_1}, \Delta Q_{ref\_1}, \ldots, \Delta P_{ref\_i}, \Delta v_{ref\_i}, \Delta Q_{ref\_i}, \ldots, \Delta P_{ref\_4}, \Delta v_{ref\_4}, \Delta Q_{ref\_4},\right]^T$, $y_{entire} = [\Delta\omega_1, \Delta\omega_2, \Delta\omega_3, \Delta\omega_4, \Delta V_{dc\_1}, \Delta V_{dc\_2}, \Delta V_{dc\_3}, \Delta V_{dc\_4},]^T$.

4. The simulation results

In order to validate the MLCCM-based small signal model, a time-domain simulation model is built in MATLAB/Simulink. The test system parameters are listed in Table 1.

Fig. 6 shows the simulation results. The results of small signal models are plotted in Fig. 6(a). While, Fig. 6(b) describes the results of time-domain simulation model. At the beginning, the AC/DC hybrid system operates at the steady state and the frequencies of AC grid is 50 Hz. Then, at $t = 0$ s, a small signal is disturbed in $\Delta \mathrm{P}_{\mathrm{ref\_1}}$, which is equivalent to a small disturbance on the active power load. The lines show the frequency fluctuations in AC grid 1. Obviously, the two line have the similar variation tendency. The response times and amplitudes are almost the same. The results demonstrate that the small signal model can reflect the dynamic response of the hybrid power system, which means the effectiveness of the proposed MLCCM modelling method.

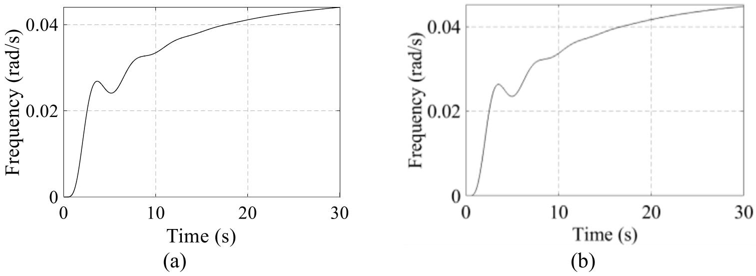

Fig. 6. Simulation results. (a) state-space model result; (b) Time-domain simulation model result.

Table 1. Parameters of test system.

Variable	Value	Variable	Value	Variable	Value	Variable	Value
S_base(MVA)	600	Kg	0.05	T_{s2}	0.03	K_{ci}	100
U_base(kV)	110	T_{G}	0.2	T_w	10	m_q	0.1
Vdc_base(kV)	400	F_{Hp}	0.3	K_{STABLE}	60	K_{d_vf}	0.0796
C_{d}(pu)	0.5333	T_{RH}	7	R_{gr}(pu)	0.0496	K_{j_vf}	10.9013
L_line(pu)	$5.1*10^{-4}$	T_{CH}	0.3	L_{gr}(pu)	$4.735*10^{-4}$	K_{fi}	0
R_line (pu)	0.04	F_{LP}	0.7	R_f(pu)	$1.438*10^{-4}$	K_{fv}	0
R_high(pu)	$5*10^{-12}$	M	1	L_f(pu)	$1.4876*10^{-4}$	K_{Qf}	62.8
R_load_1(pu)	0.7692	D	10	C_f(pu)	$2.0167*10^{-5}$	R_{dc_1}(pu)	0.0075
R_load_2(pu)	1.667	R_{g}(pu)	0.0025	K_{vp}	0.1	R_{dc_2}(pu)	0.006
R_load_3(pu)	1.667	L_{g}(pu)	0.0057	K_{vi}	10	R_{dc_3}(pu)	0.003
R_load_4(pu)	1.4286	T_{s1}	0.01	K_{cp}	1	R_{dc_4}(pu)	0.006

The eigenvalues of state matrix can be used to analyse the stability. In this paper, the eigenvalue trajectory is calculated to investigate the influence of VSC DC side capacitor (C_{dc}) on the system stability. In order to obtain a clear image, only dominant poles are shown, because 120 eigenvalue traces are too much to be shown in a clear image. Fig. 7 shows the eigenvalue traces of the state-space model (16), when the capacitance of DC capacitor decreases from 890 µF to 800 µF. It is well-known that two complex-conjugate pairs dominate the eigenvalues of oscillation frequency(2.49 rad/s). These eigenvalues are highly sensitive to the capacitance of DC capacitor. Eigenvalue analysis illustrates that the dominant poles move towards the right-half plane (unstable region) as capacitance decreases.

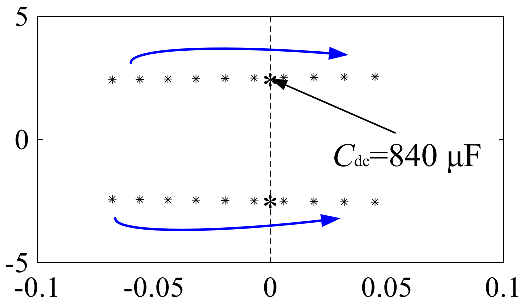

Fig. 7. Root locus with capacitance decreasing.

Fig. 8 illustrates the simulation results when the DC capacitors adopt 3 kinds of capacitance. Fig. 8 shows the frequency fluctuations of AC grid 1 in the case of a small disturbance in $\Delta P_{\mathrm{ref\_1}}$. Low frequency oscillation phenomenon occurs when the capacitance decreases to 840 µF. The simulation results demonstrate the stability analysis based on eigenvalue trajectory in Fig. 7. In other words, it validates the effectiveness of the small signal model.

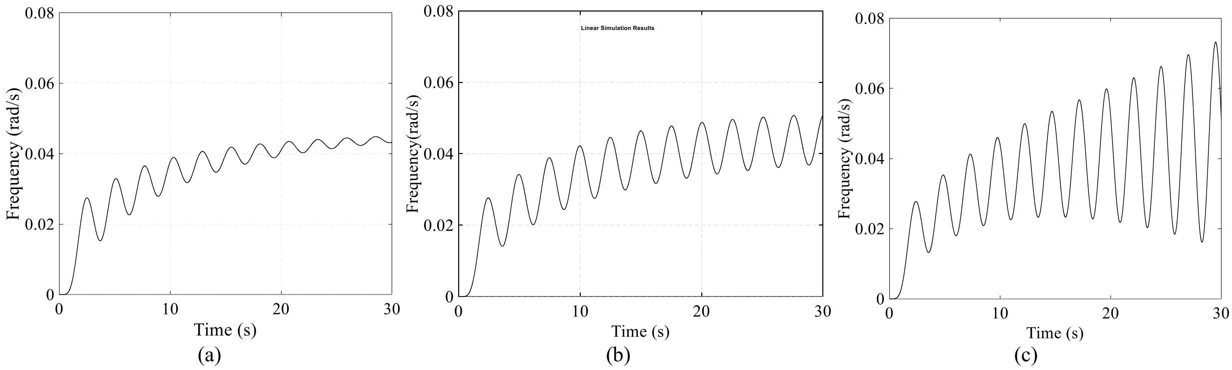

Fig. 8. Simulation results with three cases. (a) $C_{dc} = 890$ μF; (b) $C_{dc} = 840$ μF; (c) $C_{dc} = 800$ μF.

5. Conclusion

In this paper, a MLCCM is proposed for building the high order state-space model. With 120 orders, the AC/MTDC hybrid power system modelling is an example. With the help of this method, a big system can be separated into several layer subsystems or components, even though the total order is quite high. Subsystem models can be built independent, and several subsystem models are combined together by algebraic equations to build a big system model. Thus, it simplifies the modelling procedure. The compared results demonstrate the effectiveness of the method.

Declaration of competing interest

The authors declare that they have no known competing financial interests or personal relationships that could have appeared to influence the work reported in this paper.

Acknowledgement

This work was supported by the Sichuan Science and Technology Program, China under Grant 2020JDJQ0037 and 2020YFG0312.

References

[1] Leon Andres E. Short-term frequency regulation and inertia emulation using an MMC-based MTDC system. IEEE Trans Power Syst 2018;33(3):2854–63.
[2] Wang Zhenji, He Jinghan, Xu Yin, Zhang Fang. Distributed control of VSC-MTDC systems considering trade-off between voltage regulation and power sharing. IEEE Trans Power Syst 2020;35(3):1812–21.
[3] Yanbo Che, Jia Jingjing, zhou Jebei, Li Xialin, Lv Zihan, Li Ming. Stability evaluation on the droop controller parameters of multi-terminal DC transmission systems using small-signal model. IEEE Access 2019;7(2019):103948–60.
[4] Wang Yanbo, Wang Xiongfei, Chen Zhe, Frede BlaaBjerg. Small-signal stability analysis of inverter-fed power systems using component connection method. IEEE Trans Smart Grid 2018;9(5):5301–10.
[5] Du Wenjuan, Fu Qiang, Wang Haifeng. Small-signal stability of an AC / MTDC power system as affected by open-loop modal coupling between the VSCs. IEEE Trans Power Syst 2018;33(3):3143–52.
[6] Du Wenjuan, Fu Qiang, Wang Haifeng. Open-loop modal coupling analysis for a multi-input multi-output interconnected MTDC / AC power system. IEEE Trans Power Syst 2019;34(1):246–56.
[7] Rault P, Colas F, Guillaud X, Nguefeu S. Method for small signal stability analysis of VSC-MTDC grids. IEEE Power Energy Soc Gen Meet 2012;1–7.
[8] Guan Rui, Deng Na, Zhang Xiaoping. Small-signal stability analysis of the interactions between voltage source. IEEE Open Access J Power Energy 2020;7(2020):2–12.
[9] Wang Yanbo, Wang Xiongfei, Blaabjerg Frede, Chen Zhe. Harmonic stability analysis of inverter-fed power systems using component connection method. In: International power electronics and motion control conference; 2016. p. 0–7.
[10] DeCarlo RA, Sacks R. Interconnected dynamical systems. 1st ed. New York, NY, USA: Marecel Dekker, Inc; 1981.
[11] Wang Hao, Hu Weihao, Li Mingxuan, Huang Qi, Chen Zhe. Tolerant control of voltage signal fault for converter station based multi-terminal HVDC systems. IEEE Access 2019;7(2019):48175–84.
[12] Kundur P, Balu NJ, Lauby MG. Power system stability and control. 1st ed. New York, NY, USA: McGraw-Hill; 1994.